In Situ Polymerization of Poly(methyl methacrylate)/Clay Nanocomposites in Supercritical Carbon Dioxide

Qian Zhao[†] and Edward T. Samulski*[,†,‡]

Curriculum in Applied and Materials Sciences and Department of Chemistry, University of North Carolina at Chapel Hill, Chapel Hill, North Carolina 27599-3290

Received March 10, 2005

ABSTRACT: Poly(methyl methacrylate)/clay nanocomposites have been prepared using a pseudo-dispersion polymerization of MMA monomer in the presence of fluorinated surfactant-modified clay (10F-clay) in supercritical carbon dioxide. The nanocomposites are characterized by scanning electron microscopy, transmission electron microscopy, X-ray diffraction, thermal gravimetric analysis, and dynamic mechanical analysis and show partially exfoliated/intercalated structures as well as enhanced thermal stabilities, glass transition temperatures, and mechanical properties. It is also found that 10F-clay served not only as an inorganic filler but also as an effective stabilizer for PMMA polymerization in CO_2. The nature of the stabilizing mechanisms is inferred from FTIR studies. This CO_2-mediated route allows for a clean synthesis of nanocomposites with high yields without the need for extra surfactant to stabilize the system.

Introduction

Polymer/clay nanocomposites with a small percentage of layered silicates embedded in the polymer matrix are of interest because they exhibit enhanced material properties compared to the pure polymer.[1] In general, there are two idealized morphologies possible depending on the degree of polymer penetration into the clay framework: intercalated (silicate layers retain coplanar order but with their gallery distance expanded) and exfoliated (silicate layers are completely separated and disordered). Although the exfoliated structures are usually claimed to have the most significant property improvements, there are in reality very few unequivocal examples because the strong electrostatic force between clay layers tends to hold them together and underlies the preferred face-to-face stacking geometry in agglomerated clay tactoids. On the other hand, partially exfoliated nanocomposites are more readily produced having silicate layers exfoliated into secondary particles which contain several stacked, coplanar layers. Moreover, such mixtures of partially exfoliated/intercalated structures exhibit enhanced properties, i.e., high modulus and impact strength, etc,[2] especially when these secondary particles are uniformly dispersed in the polymer matrix. Typically, polymer/clay nanocomposites are prepared by direct intercalation of polymer chains from solution (solution intercalation)[3] or the molten state (melt intercalation).[4] Alternatively, intercalation of monomers into the clay gallery followed by polymerization will also disperse the silicate layers uniformly into the polymer matrix (in situ polymerization).[5] Among these methods, in situ polymerization appears to be the most promising one, pioneered by researchers from Toyota Motor Company,[5,6] who synthesized the first exfoliated nylon-6/clay hybrid for automotive applications. To render clay organophillic and more compatible with organic monomers and polymers, the sodium or calcium ions of the pristine clay are usually replaced with an alkylammonium surfactant via an ion exchange reaction. The surfactant-modified clay is used in many polymer/clay nanocomposites prepared via in situ polymerization.[7−9] However, a drawback of this method is that it usually involves large quantities of aqueous/organic solvents as the polymerization medium, which is both environmentally unfriendly and economically prohibitive for an industrial-scale application.

Supercritical carbon dioxide ($scCO_2$), on the other hand, has attracted extensive interest as a polymerization and processing medium, primarily driven by the need to replace conventional solvents with more environmentally benign and economically viable procedures.[10] However, since $scCO_2$ is a poor solvent for most hydrocarbon polymers, an effective amphiphilic stabilizer must be employed to (1) prevent coagulation of the growing polymer particles, and (2) achieve a successful dispersion polymerization. In 1994, Desimone et al. reported the first dispersion polymerization in $scCO_2$ using a CO_2-soluble fluorinated homopolymer (poly(dihydroperfluorooctyl acrylate) PFOA) as the stabilizer.[11] Since then, most of the work in this area has been focused on sophisticated stabilizers, which have ranged from fluorinated and siloxane-based block or graft copolymers,[12−14] siloxane-based macromonomers,[15] to more recent monofunctional perfluoropolyethers.[16] For each stabilizer, there are two prerequisites: (1) the stabilizer needs an anchoring segment which attaches to the monomer/polymer particle either through physical adsorption or chemical grafting; (2) a CO_2-phillic (fluorinated- or siloxane-based) segment which projects into the continuous CO_2 phase and provides steric stabilization for the growing polymer particles.

Herein, we describe a route to incorporate clays into polymer via in situ polymerization in liquid or $scCO_2$. Previous work by Zerda et al. used $scCO_2$ as a reaction medium to prepare highly filled polymer/clay nanocomposites.[17] In their work, CO_2 is primarily used to lower the viscosity resulting from high loadings (up to 40%) of clay; the clay was modified by conventional hydrocarbon surfactants and resulted in intercalated nano-

* To whom correspondence should be addressed. E-mail: et@unc.edu.
[†] Curriculum in Applied and Materials Sciences.
[‡] Department of Chemistry.

10.1021/ma050523x CCC: $30.25
Published on Web 08/16/2005

Table 1. Physical Data for Modified Clays

clays	modifying cations[a]	d spacing[b] (nm)	surfactant intercalated[c] (wt %)
Na-MMT	none	1.2	N/A
10F-clay	$CF_3(CF_2)_9(CH_2)_2Py^+$	1.4	35
12C-clay	$CH_3(CH_2)_{11}Py^+$	1.6	8
2C18-clay	$[CF_3(CH_2)_{17}]_2(CH_3)_2N^+$	3.9	40

[a] Py = pyridine. [b] Determined by XRD. [c] Determined by TGA.

composites. By contrast, our work employed much lower loadings (6 wt %) of clay, which is a typical concentration for nanocomposites. Furthermore, the clay was modified by a fluorinated surfactant in which the fluorinated tail is CO_2-phillic and thus can help provide steric stabilization in $scCO_2$. We found that the fluorinated surfactant-modified clay can itself serve as an effective stabilizer and help produce polymer in high yields in $scCO_2$. Although the clay is not soluble in CO_2, the stabilization mechanism is similar to that in a conventional dispersion polymerization. We will refer to this technique as a pseudo-dispersion polymerization.

Experimental Section

Materials. Sodium montmorrillonite (Na-MMT) was obtained from Gelest, Inc. and used as received. 1H,1H,1H,2H-Perfluorododecyl iodide was obtained from Oakwood Products, Inc. Cationic fluorocarbon surfactant 1H,1H,1H,2H-perfluorododecylpyridinium iodide was synthesized from 1H,1H,-1H,2H-perfluorododecyl iodide and pyridine according to reported methods.[18] Dodecylpyridinium chloride and dimethyldistearylammonium bromide were supplied by TCI America and used as received. Methyl methacrylate (MMA) was purchased from Aldrich Chemical Co. and purified by distillation before use. The free radical initiator 2,2-azobis(isobutyronitrile) (AIBN) was supplied by Polysciences, Inc. A very high molecular weight (M_w = 996 kDa) PMMA, used as an control, was obtained from Aldrich. Chemical Company.

Modification of Clay. A total of 1 g of Na-MMT was dispersed in 50 mL of distilled water under vigorous stirring to form a suspension. The fluorinated surfactant (1-fold cation exchange capacity of the MMT) was dissolved in 50 mL of ethanol and added to the aqueous suspension. The mixture was then stirred for 6 h between 50 and 70 °C before it was collected by filtration. The solid was subsequently washed with hot water/ethanol mixture several times until there was no white precipitate observed by an AgNO3 test, indicating an absence of halide anions. The product was then vacuum-dried at 50 °C overnight, ground into powder, and stored in a desiccator. The modified clay was denoted "10F-clay". For controls, we also modified clay with two other hydrocarbon surfactants using the same method. One is dodecylpyridinium chloride, which is the hydrocarbon analogue of the fluorinated surfactant we have synthesized; the modified clay was denoted "C12-clay". The second surfactant is dimethyldistearylammonium bromide, with which the modified clay is comparable to a commercially used clay (Cloisite 20A from Southern Clay), and it was denoted "2C18-clay".

Polymerization. Polymerizations were conducted in CO_2 in a 2.5 mL, high-pressure cell equipped with sapphire windows that allow visual observation of the mixture. In a typical polymerization, the initiator (AIBN 0.003 g) and clay (0.03 g) were weighed into the cell containing a magnetic stir bar. The cell was purged with CO_2 via an Isco automatic syringe pump (model 260D) for a few minutes, and then the monomer (0.5 mL MMA) was injected into the cell. The cell was then filled with CO_2 to ~70 bar, and heated to 65 °C. After the desired temperature was reached, the desired pressure (241 bar) was achieved by the addition of more CO_2. The reaction was allowed to proceed with stirring for 4 h, and then the cell was cooled, and the CO_2 was slowly vented. Unless specified, the final product was taken out and dried at room temperature in a vacuum oven overnight, and the resultant materials stored in a desiccator for characterization. Yields of PMMA were determined gravimetrically. For dynamical mechanical analysis, the composite was heated in a vacuum oven at 150 °C overnight to remove residual CO_2 trapped within the polymer. The sample was then pulverized and compression molded (180 °C, 54 MPa) into a thin plaque.

Table 2. Data for PMMA Obtained by Polymerizing MMA in CO_2

clays	yield (%)	$\langle M_w \rangle$ (10^3 g/mol)	sample morphologies
Na-MMT	19	472	flake
10F-clay	85	449	fine powder
12C-clay	12	364	flake/transparent paste
2C18-clay	38	392	aggregated powder/flake

Characterization. Powder X-ray diffraction (XRD) data ($2\theta = 2°$ and $2\theta = 10°$) were collected on a Rigaku multiflex diffractometer using Cu Kα radiation (40 kV, 40 mA) at a scan rate of 0.5°/min. Scanning electron microscopy (JEM6300 microscope) and transmission electron microscopy (Phillips CM12) were used to investigate the microstructure of the PMMA nancomposites. Samples for SEM were mounted on aluminum stubs using an adhesive carbon tab then gold coated. Samples for TEM were cut from the compression molded sample and thin-sectioned using a ultramicrotome (Reichert Supernova) equipped with a diamond knife. Thermogravimetric analysis (TGA) was performed using a Perkin-Elmer Pyris 1 TGA system in an argon atmosphere at a heating rate of 20 °C/min. The storage modulus and glass transition temperature of the composites were measured by a dynamic mechanical analyzer (Perkin-Elmer DMA 7e) using a extension measuring system operating at a frequency of 1 Hz; measurements were conducted in the air from room temperature to 140 °C at a scan rate of 5 °C/min. The FTIR spectra were recorded on a Fourier transform infrared spectrometer (BIO-RAD FTS 6000). Molecular weights of filtered PMMA were obtained by gel permeation chromatography (GPC) using Waters microstyragel columns (pore size 10^5, 10^4, and 10^3 Å) and a differential refractometry (Waters model 410) detector. Polystyrene standards were used for calibration.

Results and Discussion

Synthesis. Data for PMMA resulting from polymerizations of MMA in supercritical CO_2 with different clays are summarized in Table 2. Unlike typical dispersion polymerizations in which reactions start out homogeneously with a stabilizer soluble in the CO_2 phase, the pseudo-dispersion polymerizations were heterogeneous throughout the reaction due to the insolubility of clay in CO_2. The mixture formed a suspension under magnetic stirring. When 10F-clay was used, it was observed that the suspension appeared to thicken as the reaction proceeded, and precipitated powder accumulated on the cell windows during the 4 h reaction. Upon venting CO_2 at the end of the reaction, a dry powder was recovered in the form of quasispherical particles. The powder color was a little yellow to off white, since the fluorocarbon surfactant is yellow in color. The reaction exhibited a reasonably high yield (85%) with PMMA molar mass 449 KDa; this high conversion of polymer indicates a successful dispersion polymerization in CO_2. In contrast, polymerization suspensions with the two hydrocarbon surfactant-modified clays and unmodified Na-MMT were found to settle in the cell and the solution remained cloudy during the first 2 h. This probably resulted from coalescing of clay platelets covered with PMMA oligomer. As a result, polymerizations using unmodified Na-MMT and 12C-clay resulted in either flakelike morphology or transparent paste with undesirably low yields (Table 2). Although polymeriza-

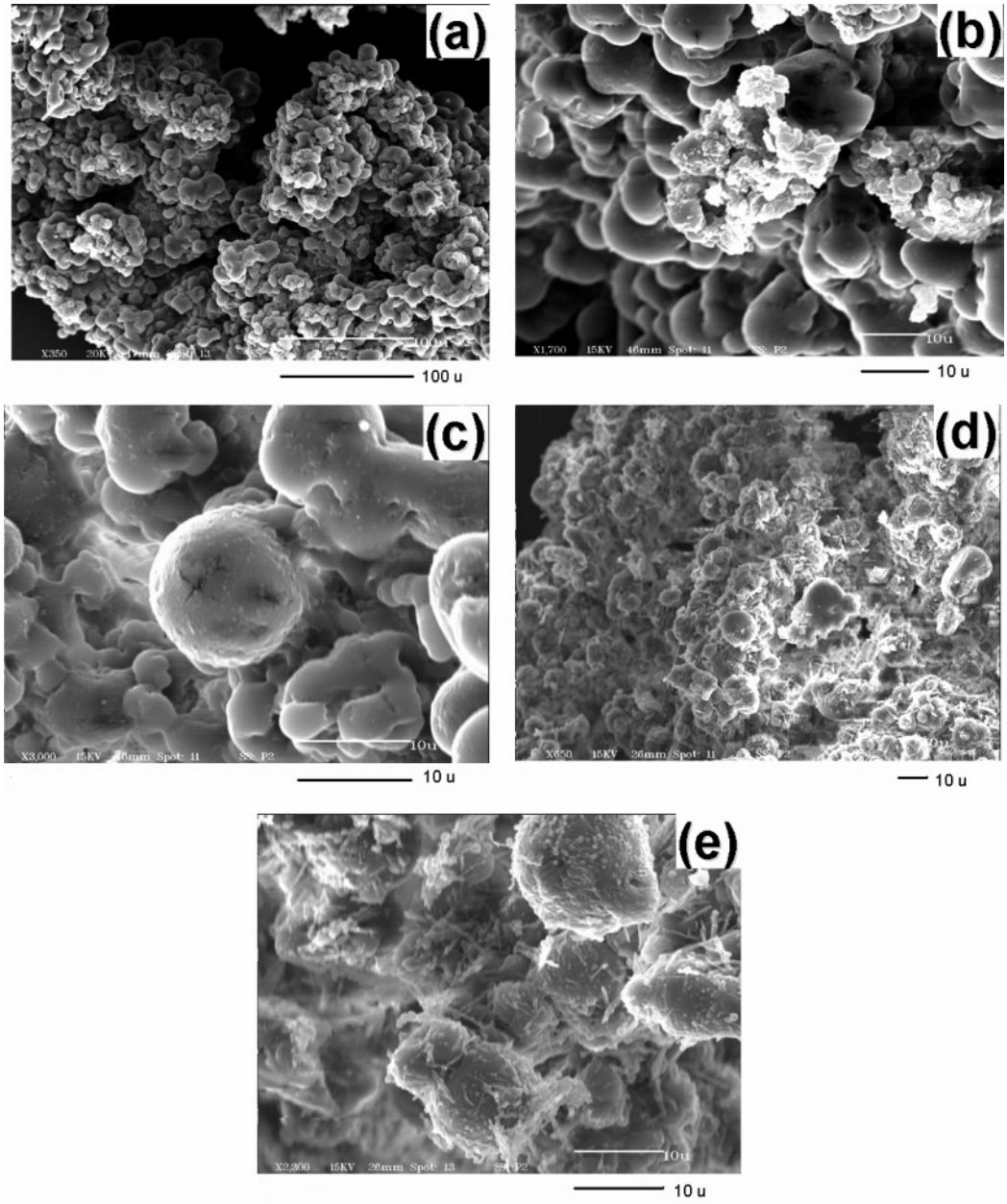

Figure 1. (a−c) SEM images of PMMA/10F-clay nanocomposites; (d and e) SEM images of PMMA/2C18-clay nanocomposites.

tion with 2C18-clay can produce a somewhat powdery PMMA, again the low yield (38%) may indicate poor stabilizing ability of the hydrocarbon surfactant-modified clay in CO_2 relative to the fluorinated surfactant-modified clay. Another interesting observation here is that the M_w's of PMMA in all of the nanocomposites, regardless of the yield, were higher than that reported for most PMMA synthesized in previous dispersion polymerizations.[19−21] GPC analysis of the PMMA extracted from clay showed a bimodal distribution with a low molecular weight shoulder for all of the nanocomposites. This phenomenon is actually not uncommon. Meneghetti et al. has explained the bimodal distribution by a "glass effect", i.e., low molecular weight PMMA becomes trapped between the clay galleries, whereas the higher molecular weight of PMMA corresponds to the amorphous matrix.[22] The higher molecular weight we observed may be attributed to the presence of clay, which can trap/scavenge free radicals and lead to an increase of molecular weight. [23]

Morphology. Analysis by SEM showed that the PMMA/10F-clay nanocomposites for the most part consisted of quasi-spherical PMMA particles (Figure 1a) with clay platelets seen adsorbed on the particle surface. The average particle diameter is about 10 μm, which is significantly larger than the typical values (a few microns) for PMMA prepared previously in dispersion polymerizations in $scCO_2$. The greater particle size may be indicative of a greater amount of agglomeration occurring during polymerization. This is probably due to the short chain length of the fluorinated surfactant and less effective steric stabilization compared with most polymeric surfactants used in conventional dispersion polymerizations.[11,13,14] Different electron densities suggest that both intercalated clay tactoids (Figure 1b) and individual exfoliated clay platelets (Figure 1c) are present on the surfaces of PMMA particles. As for the PMMA/2C18-clay nanocomposites, Figure 1d showed similar particles but the boundaries were ill-defined. The close-up image (Figure 1e) showed that there were

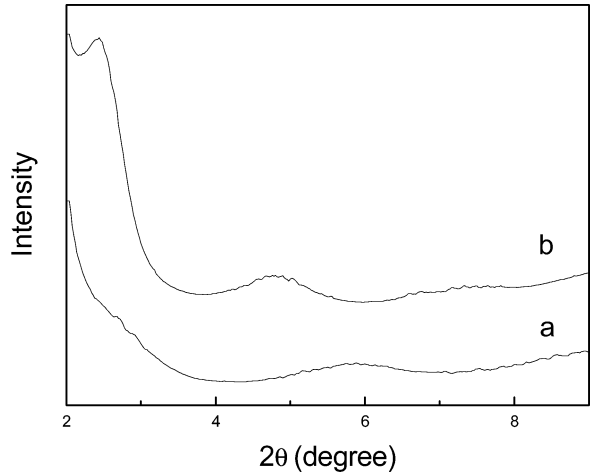

Figure 2. XRD pattern of (a) PMMA/10F-clay nanocomposites; (b) PMMA/2C18-clay nanocomposites.

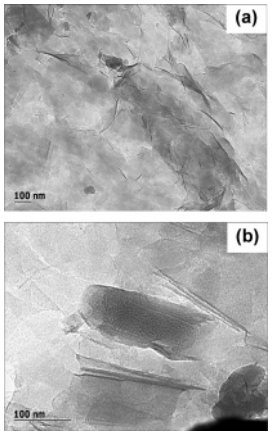

Figure 3. TEM images of PMMA/10F-clay nanocomposites (a) low magnification image showing that most of the clays layers have been exfoliated into secondary particles, and these are uniformly dispersed in the polymer matrix; (b) high magnification image showing clay tactoids containing intercalated structures.

many more clay aggregates on the PMMA particle surfaces compared with comparable images of PMMA/10F-clay nanocomposites. This further corroborates the less effective stabilizing ability of 2C18-surfactant in CO_2 compared to the fluorinated surfactant. Therefore, the growing PMMA particles need more 2C18 surfactant on the surface to provide steric stabilization in CO_2.

Figure 2 shows the XRD patterns of PMMA nanocomposites with 10F-clay and 2C18-clay. For the PMMA/10F-clay nanocomposite, the (001) peak has shifted from 1.4 nm in the 10F-clay (see Table 1) to 3.1 nm in the composite, which indicates that PMMA has intercalated into the galley of 10F-clay. Furthermore, the intensity of the diffraction peak at $d = 3.1$ nm is noticeably weaker than the strong diffraction peak ($d = 3.9$ nm) of the intercalated PMMA/2C18-clay nanocomposite. This suggests that most of the clay layers in the 10F-clay nanocomposites have exfoliated from their ordered intercalated structures, and the mixture has both intercalated and exfoliated structures.

More information about the morphology of PMMA/10F-clay nanocomposites was obtained by TEM observation. As is shown in Figure 3a, the silicate layers of clay were exfoliated into secondary particles which are uniformly dispersed in the polymer matrix. In certain areas, clay tactoids containing the intercalated structure

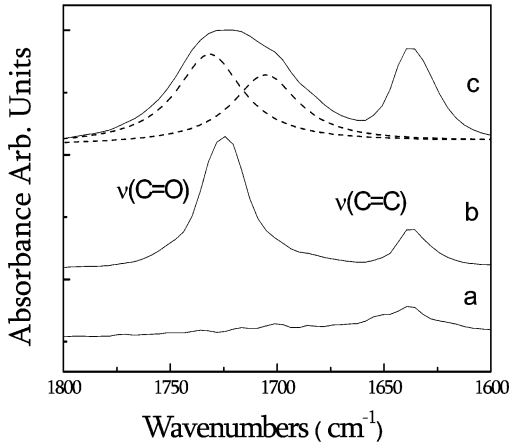

Figure 4. FT-IR spectra of (a) 10F-clay; (b) MMA; (c) mixture of 10F-clay and MMA.

can still be seen. (Figure 3b). This further supports the SEM observations and XRD analysis which suggested that partially exfoliated and partially intercalated nanocomposites were formed.

Stabilization Mechanism. It is clear that the 10F-clay is not only acting as an inorganic filler but also as a stabilizer for PMMA growth in CO_2. From SEM observations, we propose that it is the individual clay platelets which absorb on the surface of the PMMA particles that provide the stabilization mechanism in CO_2. Evidence for the anchoring mechanism is provided by FT-IR spectroscopy. As is shown in Figure 4, pure MMA has the carbonyl stretching mode at 1725 cm^{-1}, whereas 10F-clay is silent in this region except for a H−O−H deformation band around 1635 cm^{-1}. However, when MMA is mixed with 10F-clay, the carbonyl stretching band is apparently broadened (Figure 4c). The broadened band can be deconvoluted into two bands: One band (unreacted carbonyl stretch) remains about the same position, whereas the other shifts to lower frequency by 20 cm^{-1}. Such a shift is indicative of a hydrogen bond interaction, which is a typical phenomenon when carbonyl containing compounds are adsorbed onto swelling clay minerals. It has been proposed that the C=O group is either bound to the exchangeable cation through a water molecule bridge (i.e., a hydrogen bond) or it is directly linked to the metallic cation.[24] Here, since most of the metallic cations in our clay have been exchanged with fluorinated surfactant, the interaction is most likely the first one, hydrogen bonding between the C=O group and the interlayer water of the partially hydrated clay.

Thermal Properties. Figure 5 shows the TGA curves of pure PMMA, PMMA/10F-clay nanocomposites, and PMMA/2C18-clay nanocomposites. As is shown in curves b and c, the small weight loss between 100 and 150 °C can be attributed to evaporation of residual MMA monomers from the in situ polymerized nanocomposites. Apparently, the onset of decomposition temperature of PMMA/10F-clay has increased from that of both pure PMMA and PMMA/2C18-clay; this is probably due to the barrier properties of the partially exfoliated 10F-clay in the polymer matrix, retarding the escape of decomposition products. As the temperature further increases above 350 °C, MMA/2C18-clay nanocomposites tend to have a slightly higher ending decomposition temperature than that of PMMA/10F-clay. A possible reason is that the weight percentage of 2C18-clay in the nanocompoistes is higher than that of 10F-clay due to

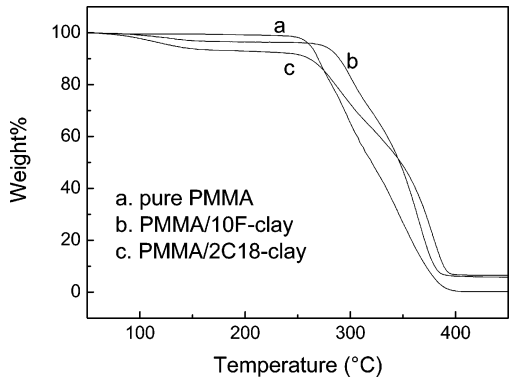

Figure 5. TGA curves of (a) pure PMMA; (b) PMMA/10F-clay nanocomposite; (c) PMMA/2C18-clay nanocomposite.

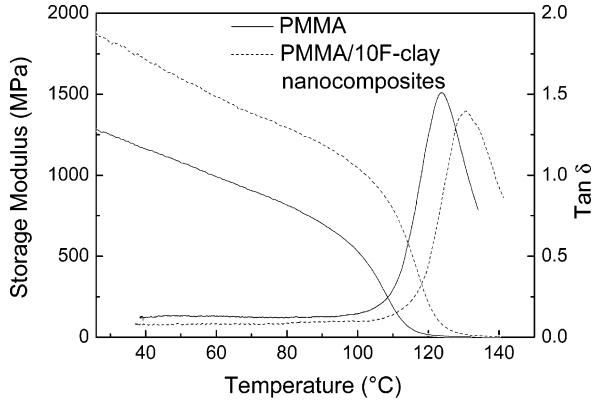

Figure 6. Storage modulus and loss tangent (tanδ) spectra of PMMA and PMMA/10F-clay nanocomposites.

the lower yield of polymer. That is, the higher concentration of the inorganic filler may play a role in enhancing the thermal stability of the polymer.

Mechanical Properties. Dynamic mechanical analysis was used to measure the viscoelastic properties of the polymer nancomposites. Figure 6 shows the temperature dependence of storage modulus and tan δ of PMMA and PMMA/10F-clay nanocomposites. As expected, the storage modulus increases with the addition of clay: at 26 °C, the modulus increases from 1.28 GPa for PMMA to 1.88 GPa for the nanocomposite. An enhanced glass transition temperature ($T_g = 132$ °C for the nancomposites versus $T_g = 124$ °C for PMMA) corresponding to the peak of the loss tangent is also observed for the PMMA/10F-clay nanocomposites. It has been suggested[9,25] that the enhancements of the storage modulus and glass transition temperature result from the strong interfacial interactions between the polymer and clay, the restricted segmental motions of polymer chains at the organic−inorganic interface, and the inherent high modulus of the clays.

Conclusions

PMMA/clay nanocomposites have been synthesized via a novel pseudo-dispersion polymerization technique in $scCO_2$. It has been found that the fluorinated surfactant-modified clay (10F-clay), although not soluble in CO_2, can indeed serve as an effective stabilizer for PMMA polymerization in CO_2 and help improve polymer yields compared with conventional hydrocarbon surfactant-modified clay. The mechanism is most likely that the fluorinated surfactant provides steric stabilization in the CO_2 phase, whereas the clay itself interacts with the carbonyl group of the methacrylate moiety via hydrogen bonding. The nanocomposites were characterized by SEM, TEM, XRD, TGA, and DMA and showed partially exfoliated/intercalated structures as well as enhanced thermal stabilities, glass transition temperatures, and mechanical properties. This pseudo-dispersion polymerization route allows for clean synthesis of nanocomposites with high yields in $scCO_2$, without the need for adding extra surfactant to stabilize the polymerization system.

Acknowledgment. This work was supported in part by NASA Grant (NAG-1-2301) and used NSF-STC shared equipment facilities. We thank Dr. Wallace Ambrose for assistance in TEM sample preparation, Prof. O. Zhou for the use of TGA and DMA instrumention, and Prof. J. DeSimone for helpful discussions.

References and Notes

(1) Lebaron, P. C.; Wang, Z.; Pinnavaia, T. J. *Appl. Clay Sci.* **1999**, *15*, 11−29.
(2) Manias, E. *MRS Bull.* **2001**, *26*, 862−863.
(3) Wu, J.; Lerner, M. *Chem. Mater.* **1993**, *5*, 835−838.
(4) Vaia, R.; Vasudevan, S.; Krawiec, W.; Scanlon, L.; Giannelis, E. *Adv. Mater.* **1995**, *7*, 154−156.
(5) Kojima, Y.; Usuki, A.; Kawasumi, M.; Okada, A.; Kurauchi, T.; Kamigaito, O. *J. Polym. Sci., Part A: Polym. Chem.* **1993**, *31*, 983−986.
(6) Usuki, A.; Kojima, Y.; Kawasumi, M.; Okada, A.; Fukushima, Y.; Kurauchi, T.; Kamigaito, O. *J. Mater. Res.* **1993**, *8*, 1179−1184.
(7) Ma, J.; Qi, Z.; Hu, Y. *J. Appl. Polym. Sci.* **2001**, *82*, 3611−3617.
(8) Messersmith, P.; Giannelis, E. *J. Polym. Sci., Part A: Polym. Chem.* **1995**, *33*, 1047−1057.
(9) Okamoto, M.; Morita, S.; Taguchi, H.; Kim, Y.; Kotaka, T.; Tateyama, H. *Polymer* **2000**, *41*, 3887−3890.
(10) Shaffer, K.; Desimone, J. *Trends Polym. Sci.* **1995**, *3*, 146−153.
(11) Desimone, J.; Maury, E.; Menceloglu, Y.; Mcclain, J.; Romack, T.; Combes, J. *Science* **1994**, *265*, 356−359.
(12) Canelas, D.; Desimone, J. *Macromolecules* **1997**, *30*, 5673−5682.
(13) Hems, W.; Yong, T.; Van Nunen, J.; Cooper, A.; Holmes, A.; Griffin, D. *J. Mater. Chem.* **1999**, *9*, 1403−1407.
(14) Lepilleur, C.; Beckman, E. *Macromolecules* **1997**, *30*, 745−756.
(15) Shaffer, K.; Jones, T.; Canelas, D.; Desimone, J.; Wilkinson, S. *Macromolecules* **1996**, *29*, 2704−2706.
(16) Christian, P.; Howdle, S.; Irvine, D. *Macromolecules* **2000**, *33*, 237−239.
(17) Zerda, A.; Caskey, T.; Lesser, A. *Macromolecules* **2003**, *36*, 1603−1608.
(18) Asakawa, T.; Hisamatsu, H.; Miyagishi, S. *Langmuir* **1995**, *11*, 478−482.
(19) Yates, M.; Li, G.; Shim, J.; Maniar, S.; Johnston, K.; Lim, K.; Webber, S. *Macromolecules* **1999**, *32*, 1018−1026.
(20) Christian, P.; Giles, M.; Griffiths, R.; Irvine, D.; Major, R.; Howdle, S. *Macromolecules* **2000**, *33*, 9222−9227.
(21) Yong, T.; Hems, W.; Vannunen, J.; Holmes, A.; Steinke, J.; Taylor, P.; Segal, J.; Griffin, D. *Chem. Commun.* **1997**, 1811−1812.
(22) Meneghetti, P.; Qutubuddin, S. *Langmuir* **2004**, *20*, 3424−3430.
(23) Solomon, D. H.; Swift, J. D. *J. Appl. Polym. Sci.* **1967**, *11*, 2567
(24) Yariv, S.; Cross, H. *Organo-Clay Complexes and Interactions*; Marcel Dekker: New York, 2002.
(25) Mcnally, T.; Murphy, W. R.; Lew, C.; Turner, R.; Brennan, G. *Polymer* **2003**, *44*, 2761−2772.

MA050523X